
Article:
Ma, J., Dong, Z., Otitoju, O. orcid.org/0000-0001-7658-1049 et al. (3 more authors) (2024) Heat integration, process design and techno-economic assessment of post-combustion carbon capture using piperazine for large-scale ethylene plant. Chemical Engineering Science, 284. 119531. ISSN 0009-2509

https://doi.org/10.1016/j.ces.2023.119531

Heat Integration, Process Design and Techno-Economic Assessment of Post-Combustion Carbon Capture Using Piperazine for Large-Scale Ethylene Plant

Jin Ma[a], Zhaoxi Dong[a], Olajide Otitoju[b], Meihong Wang[a,b,*], Wenli Du[a], Feng Qian[a]

[a] Key Laboratory of Smart Manufacturing in Energy Chemical Process, Ministry of Education, School of Information Science and Engineering, East China University of Science and Technology, Shanghai 200237, China

[b] Department of Chemical and Biological Engineering, The University of Sheffield, Sheffield S1 3JD, United Kingdom.

* Corresponding Author: Meihong Wang

Tel: +44(0) 114 222 7160

E-mail: Meihong.Wang@sheffield.ac.uk

Abstract

With the development of increasingly larger ethylene plants and the associated requirement to reduce carbon emissions effectively, there is a growing need to explore approaches that reduce the cost and energy consumption in carbon capture from ethylene plants. In this study, the flue gas heat recovery (FHR) strategy was proposed and implemented for different configurations of piperazine (PZ)-based post-combustion carbon capture (PCC) process applied to an ethylene plant with a capacity of 60,000t/year. Four different cases of the PZ-based PCC process with or without FHR were simulated in Aspen Plus® V11 to explore the cost reductions and energy saving potential. The advanced flash stripper (AFS) configuration with FHR and absorber inter-cooling achieves a minimum regeneration energy requirement of 2.28 GJ/tonCO_2, a reduction of 37.71% compared to standard PCC configuration using MEA solvent. The economic evaluation was carried out using Aspen Process Economic Analyzer® (APEA). The results show that the carbon capture cost using AFS configuration with FHR and inter-cooling can reduce to 47.27 \$/tonCO_2, a reduction of 36.76% against the standard PCC process using MEA. The proposed technology presents significant technical and economic benefits for the large-scale deployment of carbon capture for ethylene plants.

Keywords: Post-combustion carbon capture, Chemical absorption, Piperazine, Rate-based simulation, Heat recovery, Techno-economic assessment

1. Introduction

1.1 Background

~~The energy intensive chemical industry produces 16% of direct global carbon emissions with responsibility for climate change (Takht and Sahebdelfar, 2014).~~ The energy-intensive chemical industry produces 5% of global direct carbon emissions (about 2 billion metric tons of CO_2) and is responsible for climate change (Gabrielli et al., 2023). As one of the most important building blocks of the chemical industry, the production capacity of the ethylene manufacturing process in China is increasing every year to cut down the gap between supply and demand (Zhao et al., 2018). A doubling of ethylene production capacity from 35.2 million tonnes in 2022 to 73.5 million tonnes in 2025 has been predicted (China Petroleum and Chemical Industry Association, 2022). The carbon footprint for an ethylene plant is estimated to be about 1.56 tons per ton of ethylene produced (Keller et al., 2020). More than 80% of this is contributed by direct emission from the combustion of fuel in the thermal cracking furnaces, which is the heat of the ethylene production process (Mynko et al., 2022). Therefore, it is essential to implement a carbon capture process for short and mid-term carbon emission reduction from ethylene plants (Wang et al., 2011).

The solvent-based post-combustion carbon capture (PCC) is the most promising carbon capture method for the decarbonization of ethylene plants. However, the major barriers to this technology are high energy consumption and high costs. (Wang et al., 2015) To address these issues, several options have been explored which include the use of alternative solvents such as Piperazine (PZ) to replace the commonly used Monoethanolamine (MEA) (Rochelle et al.,

2011) and the use of new process configurations such as the absorber inter-cooling and Advance flash stripper (AFS) in place of the standard process configurations (Rochelle et al., 2019). This paper builds on these improvements by implementing a flue gas heat recovery (FHR) strategy and investigates the energy and cost reduction potential of this strategy on a PZ-based PCC process capturing CO_2 from the flue gas of a 60 kt/a ethylene plant.

1.2 literature review

MEA is a primary amine that reacts with carbon dioxide in the liquid phase, and it has been extensively studied as a mature solvent for the PCC process. The rigorous rate-based modelling of the PCC process using 30 wt% MEA has been implemented for coal-fired power plants (Lawal et al., 2010; Lawal et al., 2012), combined cycle gas turbine (CCGT) power plants (Canepa et al., 2013, Otitoju et al., 2021) and the refinery fluid catalytic cracking unit (FCCU) (Wei et al., 2018). Although MEA has the advantages of low price, fast reaction, relatively low viscosity, however, it degrades at temperatures, is susceptible to pollutants such as NOx, SO_2 and O_2 and consumes high energy for regeneration. For instance, an MEA-based PCC process deployed in a 60,000t/year ethylene production plant requires 3.82 GJ of energy and cost $74.75 to capture one tonne of CO_2 (Hu et al., 2023). These high energy and cost requirements are obstacles to rapid commercial deployment of the process.

Thus, various new solvents with better properties and faster reaction rates than MEA have been developed and used for the PCC process (Li et al., 2014; Nwaoha et al., 2017; Na et al., 2019; Jin et al., 2021; Luo et al., 2022; Chen et al., 2023). A new amine solvent CESAR1 reduces regeneration consumption by 20% and solvent flowrate by 45% compared to MEA

(Mangalapally and Hasse, 2011). Ionic liquids have also been investigated as solvents for PCC given their high absorption capacity, stability and negligible volatility (Zhou et al., 2021).

One of the attractively used absorbents is PZ (Freeman et al., 2010), which was initially usually used in combination with MDEA (Zhao et al., 2017) and K_2CO_3 (Arsbad et al., 2014). As the low volatility (Nguyen et al., 2010), low corrosion (Liu et al., 2020), thermal degradation (Freeman et al., 2010) and high absorptive capacity (Dugas and Rochelle, 2011) of PZ aqueous solutions are gradually being explored, it is becoming a favoured option for carbon capture process studies. A comparison of the performance of 40 wt% PZ and 30 wt% MEA is shown in **Fig.1**.

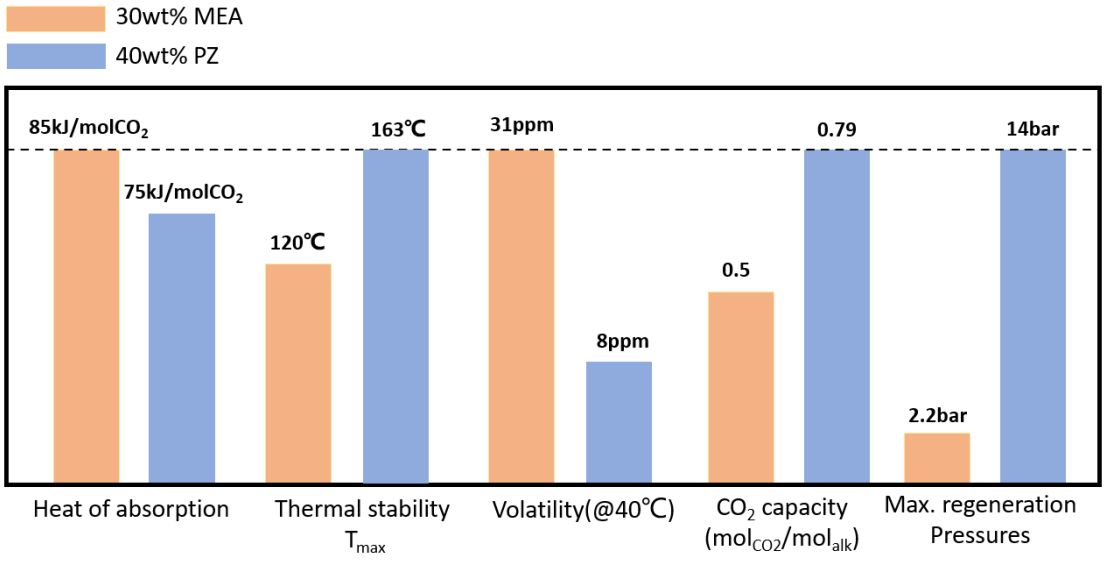

Fig.1 Comparison of the performance of 40 wt% PZ and 30 wt% MEA (Kim and Svendsen, 2007; Frailie et al.,2014; Li et al., 2013)

PZ is a diamine and 1mole PZ contains 2mole of alkalinity. CO_2 loading is generally defined as the moles of CO_2 per mole alkalinity (i.e. 0.5 moles PZ) (Plaza, 2011). Despite its many advantages, PZ hydrates are formed at low CO_2 loadings. 40 wt% PZ solvent form solids when the CO_2 loading is too high or too low (Chen et al., 2017). The variation of 40 wt% PZ solubility with CO_2 loading is displayed in **Fig.2**. Concerning the practical operating conditions

of the pilot plant and simulation studies using PZ solvent (Chen et al., 2017; Babu et al., 2022), the operating range of CO_2 loading was selected to be 0.2 to 0.4 mol_{CO2}/mol_{alk} to avoid operational problems.

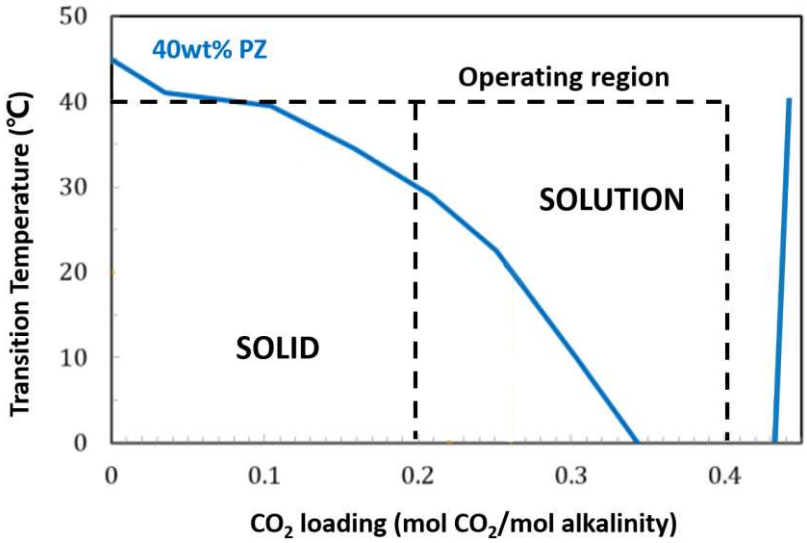

Fig.2 Solubility of aqueous solutions of PZ (Chen et al., 2017)

PZ solvent have been employed successfully in several pilot plants tests, such as the J.J pickle facility pilot plant at the University of Texas at Austin, USA (Chen et al., 2017; Van Wagener, 2011), and the CO2SEPPL program at the EVN power plant in Austria (Rabensteiner et al., 2015). Some studies have also investigated the deployment of PZ-based PCC processes for coal-fired power plants (Frailie et al.,2014) and natural gas combined cycle (NGCC) power plants (Otitoju et al., 2021). It is reported that the solvent-based PCC process using 40 wt% PZ can reduce energy consumption by 9%~11% compared to 40 wt% MEA (Van Wagener and Rochelle, 2011).

With the further pursuit of energy saving, two process improvements, inter-cooling (Gao and Rochelle, 2022) and the advanced flash stripper (AFS), were developed and applied (Zhang et al., 2017; Guo, 2021; Babu and Rochelle, 2022). Retrofitting the absorber with an intercooler

unit can reduce packing requirements and solvent costs (Gao and Rochelle, 2019). In-and-out inter-cooling is more effective at high CO_2 concentrations, and pump-around inter-cooling is more suitable for low CO_2 concentrations (Zhang et al., 2016). Rochelle used the PZAS™ (Piperazine with the Advanced Stripper) process to conduct a 2,000 hours pilot test of CO_2 capture from NGCC flue gas with 30 wt% PZ solution (Rochelle et al., 2022). The energy consumption for solvent regeneration is 2.45 GJ /ton CO_2. The study also showed that the use of absorber inter-cooling is reliable for CO_2 capture from the flue gas. It was further established that using PZ as a solvent could lead to a smaller absorber size in the PCC process. The pilot test of the PCC process using PZ solvent and AFS conducted by the University of Texas Separations Research Program (UT-SRP) in March 2015 reported an energy consumption in the range of 2.1~2.5 GJ per tonne CO_2 for the process (Lin et al., 2016).

1.3 Novelty

This paper has the following novel contributions:

- This study proposed to use different solvents for carbon capture in ethylene plants.

Previous simulation studies focused on CO_2 capture for power plants and refineries (Wei et al., 2018; Otitoju et al., 2021). However, due to the expansion of ethylene manufacturing and the large amount of carbon emissions associated with it, it is therefore imperative to study the large-scale PCC process for an ethylene plant. In this study, based on the flue gas from the thermal cracking furnace, the PCC process for a 60,000t/year ethylene plant was simulated in Aspen Plus®. Previous studies on carbon capture in ethylene plants have been mainly on PCC processes using MEA solvent (Hu et al., 2023). Carbon capture using different solvents for

ethylene plant is yet to be investigated. In this work, the alternative solvent (PZ) was used for PCC process in ethylene plants.

- FHR is proposed for energy saving and capture cost reduction.

Previous studies ignoring the potential for PCC process with FHR. Recovery of flue gas waste heat is a straightforward energy saving scheme. Previous research regarding flue gas waste heat recovery has focused on implementation through heat pumps (Alabdulkarem et al., 2015), however, the economics of this approach has yet to be investigated. By analysing carbon capture process, it was identified that FHR can be implemented in the form of heat exchange with rich solvent. Therefore, in this paper, FHR strategy was proposed for carbon capture.

- Techno-economic assessment to analyse contribution from different factors in cost reduction and energy saving.

In this study, the PZ-based PCC process using different configurations (e.g. AFS and\or inter-cooling) with FHR is simulated and the techno-economic assessment is performed. The results show a 36.76% reduction in capture cost and a 37.71% reduction in energy consumption compared to standard carbon capture using MEA. These significant reductions were caused by the change of solvent (from 30 wt% MEA to 40 wt% PZ), FHR and configuration improvements (with AFS and inter-cooling), and the contributions of these factors were also quantified.

2. Process description

2.1 Process description of thermal cracking furnace

The thermal cracking furnace, which cracks the feedstock to ethylene and propylene at high temperatures, is the most important equipment in the ethylene manufacturing process and

the primary source of carbon emissions in an ethylene plant.

The thermal cracker is divided into the outside (flue gas side) and inside (cracked feedstock side) of the reactor tube. On the flue gas side of the thermal cracking furnace, the fuel gas and air first enter the combustion chamber through burners and the majority of the energy generated by the fuel gas combustion is used to heat the reactor tubes in the radiation section. The residual energy is recovered by preheating the cracking feedstock and exchanging it with the boiler feed water to the steam drum and the high-pressure steam leaving the steam drum in the convection section. The flue gas outlet temperature at the outlet of the convection section is eventually decreased to approximately 120°C. A typical diagram of the industrial thermal cracking furnace is shown in **Fig.3**.

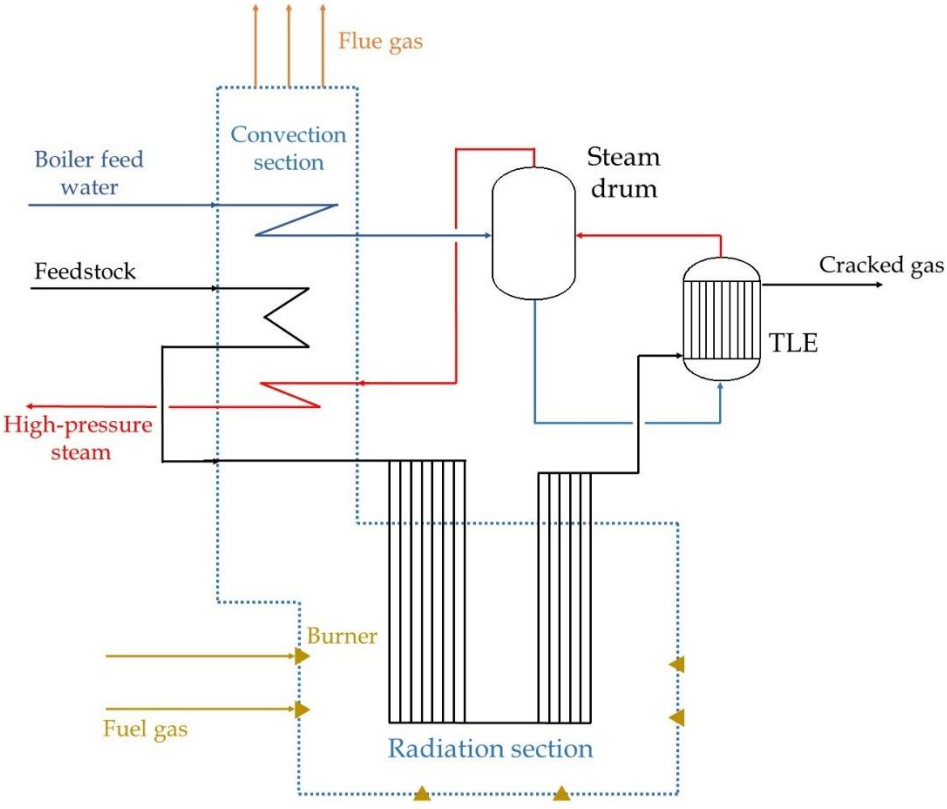

Fig.3 A typical diagram of the industrial steam cracking furnace (Hu et al., 2023)

The composition, temperature, pressure and mass flowrate of the flue gas at the outlet of

the convection section of the thermal cracking furnace are obtained from Hu et al. (2023) and are shown in **Table 1**.

Table 1. Simulated results of outlet flue gas

Variable	Value
Outlet temperature (°C)	115.5
Outlet pressure (bar)	1.01
Flowrate (kg/s)	24.72
Mole composition	
O_2 (mol%)	3.87
H_2O (mol%)	15.6
CO_2 (mol%)	7.69
N_2 (mol%)	72.84

2.2 Process description of the PCC process

2.2.1 Process description of standard PCC process

The standard configuration of the PCC process using PZ is shown in **Fig.4**. It contains an absorber, a stripper, a heat exchanger, a pump and a compression unit. Flue gas from the upstream equipment is fed into the bottom of the absorber after cooling to 40°C and removing excess water. In the absorber, about 90% of the CO_2 in the flue gas is absorbed by the PZ solvent, the rich solvent is then heated by the cross-heat exchanger and pumped to the stripper for regeneration. The captured CO_2 is compressed for transportation and geological storage. The standard configuration serves as a benchmark to which other configurations are compared.

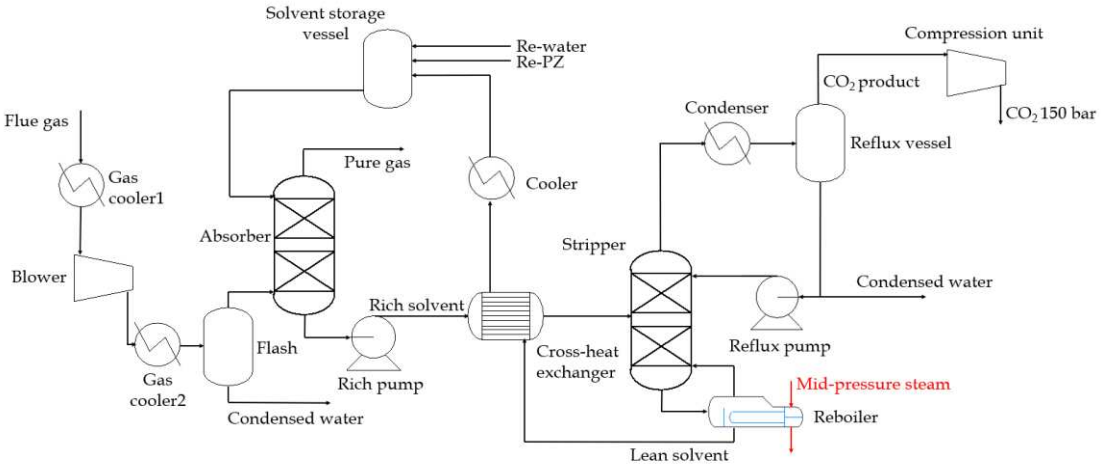

Fig.4 Standard PCC process configuration (Wu et al., 2020)

2.2.2 Process description of absorber inter-cooling configuration

The absorber inter-cooling process configuration involves adding an intercooler and a pump to the absorber in the standard configuration as shown in **Fig.5**. Due to the solvent temperature increase during the exothermic absorption process, the mass transfer process is limited as the solvent absorption capacity decreases. The absorber inter-cooling unit improves the mass transfer capacity by lowering the temperature of the liquid phase in the absorber thereby reducing the required solvent flowrate in the PCC process. This results in the potential to reduce the size of absorber and the energy consumption for solvent regeneration.

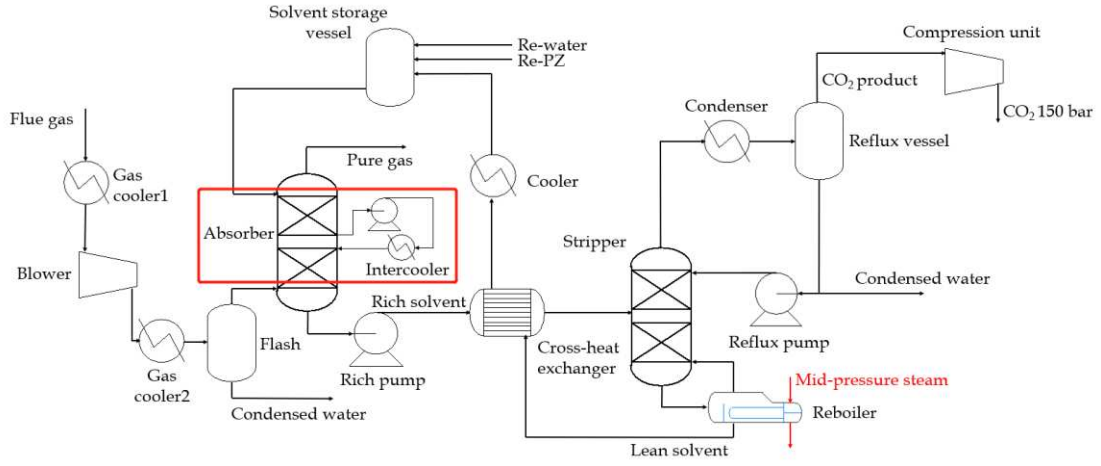

Fig.5 Absorber inter-cooling configuration of the PCC process (Biliyok et al., 2012)

2.2.3 Process description of AFS configuration

The innovative AFS configuration proposed and tested at a pilot scale (Lin et al., 2016) is shown in **Fig.6**. It is different from the standard configuration. The rich solvent from the absorber is split twice. A cold-rich bypass in the first split recovered the heat of the vapour phase from the top of the stripper, and the residual rich solvent was pre-heated by the lean solvent from the stripper in the cold cross-exchanger and transported into a hot-rich bypass. This hot-rich bypass was split once more. A portion of this hot-rich bypass is fed to the top of the stripper. The residual hot-rich solvent was further heated by the lean solvent and hot steam in the hot cross-exchanger and steam heater respectively and sent to the flash tank at the bottom of the stripper.

The energy consumption reduction of the AFS configuration was due to the recovery of the latent heat of water in the stream exiting the top of the stripper. In addition, the stripper regeneration consumption could be reduced by optimizing the separation ratio of the two splits. In the AFS configuration, the reboiler of the standard stripper is replaced with the steam heater and the flash tanks.

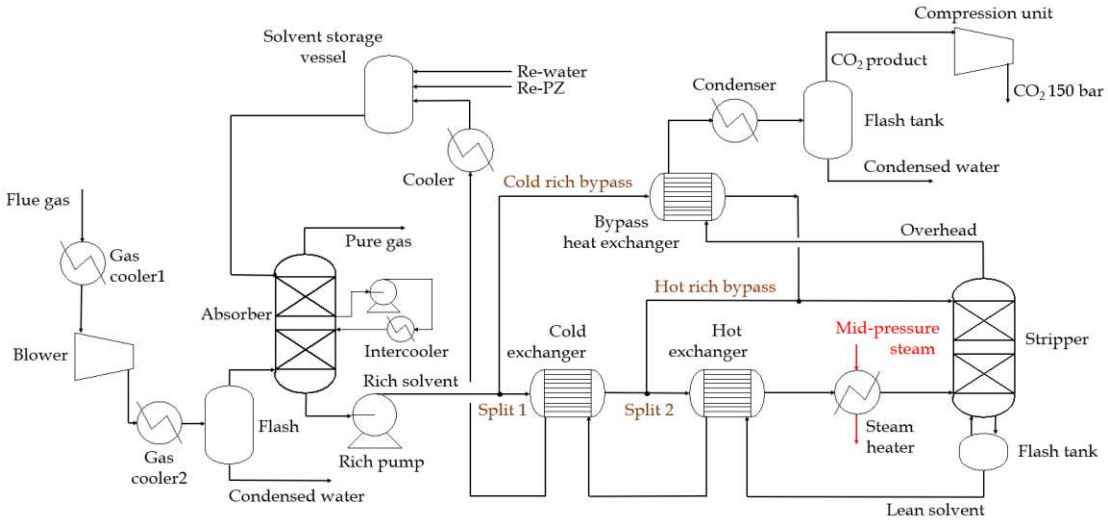

Fig.6 The AFS configuration of the PCC process using PZ (Lin et al., 2016)

2.3 Process description of proposed FHR

The temperature of the flue gas from upstream of the PCC process is generally around 120℃. The low water content and thereby low dew point temperature make it difficult to employ the latent heat. Many studies have attempted to utilize this energy through heat pumps (Alabdulkarem et al., 2015), however, the economics of this approach has yet to be investigated.

The heat requirements for the PCC process shown in **Fig.7** can provide a novel glimpse into the utilization of flue gas waste heat. The main heat demand unit of the carbon capture system is the reboiler, which is maintained at a temperature of about 115℃ and needs to be heated with steam at 125℃ or higher, and flue gas waste heat cannot meet this requirement.

Another area of the carbon capture system that requires a lot of heat is the rich solvent, which needs to be heated from 50℃ to about 100℃ before entering the top of the stripper. The flue gas waste heat can be used to raise the temperature of the rich solvent by exchanging heat with each other. This creates a new way of FHR. The schematic of the standard PCC process with FHR is shown in **Fig.8**.

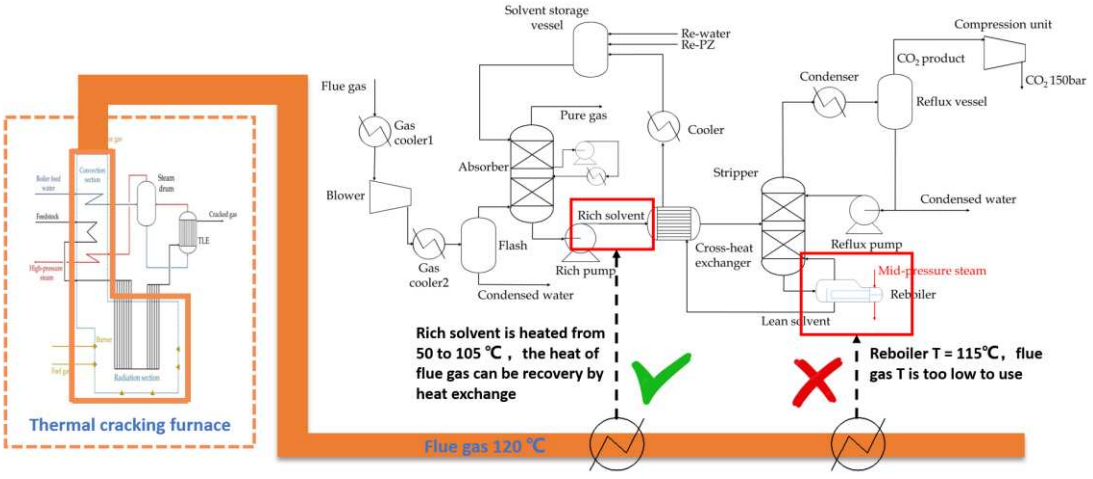

Fig.7 Two choices for FHR

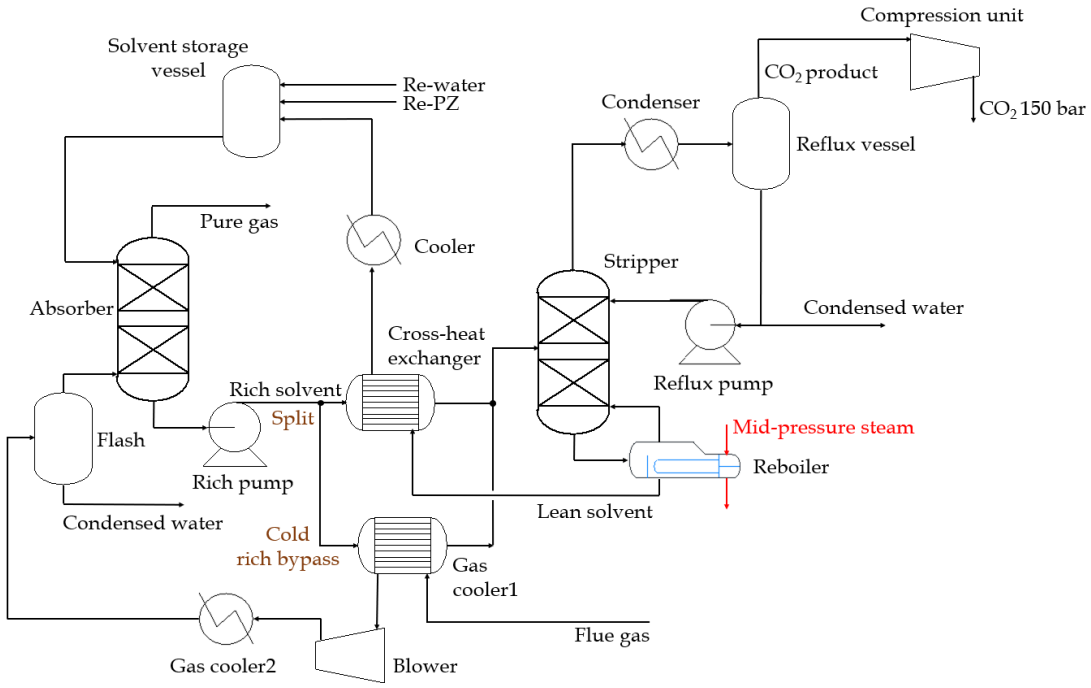

Fig.8 The configuration of the standard PCC process with FHR

3. Model development and model validation of PCC at pilot scale

3.1 model development

The thermodynamics and kinetics of carbon capture using PZ solvent have been studied (Cullinane and Rochelle, 2006; Dugas and Rochelle, 2009; Frailie et al., 2011; Akinpelumi et al., 2019). ~~In this study, the PCC process model using PZ was developed in Aspen Plus® V11.~~ In this study, the information related to solubility, volatility and heat capacity based on experimental data that has been reported was used in developing CO_2 capture process using PZ in Aspen Plus® V11. Both the absorber and stripper are simulated using the rate-based model in the RadFrac block. Rate-based models provide a rigorous unit operation model and correlation of physical properties and reactions and have been proven to be superior to the equilibrium-based model. The physical property of the liquid phase was calculated using the

Electrolyte Non-Random Two-Liquid (ElecNRTL) thermodynamic method and that of the vapour phase was calculated using the Redlich-Kwong equation of state. The choice of certain correlations and coefficients is specifically stated below. The molar volume of the liquid mixture was calculated using the Rackett model (Rackett, 1970). The viscosity of the liquid mixture was obtained by the Jones-Dole electrolyte model (Horvath, 1985). The thermal conductivity of the liquid mixture was computed using Sato-Riedel and Vredeveld model for molecules and Riedel correction for electrolytes (Aspen Tech, 2020). Wilke-Chang model was applied to calculate the effective diffusion coefficient of a component in the liquid mixture (Wilke and Chang, 1955). Mixture surface tension was calculated using the Hakim-Steinberg-Stiel model for molecules with Onsager-Samaras electrolyte correction (Horvath, 1985).

The equilibrium reactions describing the chemistry of CO_2 absorption using PZ solvent are as follows:

$$2H_2O \leftrightharpoons H_3O^+ + OH^- \quad (1)$$

$$CO_2 + 2H_2O \leftrightharpoons HCO_3^- + H_3O^+ \quad (2)$$

$$H_2O + HCO_3^- \leftrightharpoons CO_3^{2-} + H_3O^+ \quad (3)$$

$$PZH^+ + H_2O \leftrightharpoons PZ + H_3O^+ \quad (4)$$

$$PZ + HCO_3^- \leftrightharpoons PZCOO^- + H_2O \quad (5)$$

$$H^+PZCOO^- + H_2O \leftrightharpoons PZCOO^- + H_3O^+ \quad (6)$$

$$PZCOO^- + HCO_3^- \leftrightharpoons PZ(COO^-)_2 + H_2O \quad (7)$$

The general expression of temperature-dependent equilibrium constants (Keq) for equilibrium reactions based on the molar concentration scale is presented in Eqs.8. The

243 coefficients for calculating the equilibrium constant of Eqs.1-7 have been experimentally
244 obtained and reported and are publicly available (Posey and Rochelle, 1997; Hetzer et al., 1968;
245 Ermatchkov et al., 2003; Xia et al. 2003; Kamps et al., 2001).

246 $$In\ K_{eq} = A + \frac{B}{T} + CInT + DT \tag{8}$$

247 The rate-controlled reactions are shown in Eqs.9-14.

248 $$CO_2 + OH^- \rightarrow HCO_3^- \tag{9}$$

249 $$HCO_3^- \rightarrow CO_2 + OH^- \tag{10}$$

250 $$PZ + CO_2 + H_2O \rightarrow PZCOO^- + H_3O^+ \tag{11}$$

251 $$PZCOO^- + H_3O^+ \rightarrow PZ + CO_2 + H_2O \tag{12}$$

252 $$PZCOO^- + CO_2 + H_2O \rightarrow PZ(COO^-)_2 + H_3O^+ \tag{13}$$

253 $$PZ(COO^-)_2 + H_3O^+ \rightarrow PZCOO^- + CO_2 + H_2O \tag{14}$$

254 The kinetic expression of reactions 9-14 governed by the power law is represented in
255 Eqs.15.

256 $$r = A\ exp\left(-\frac{E}{RT}\right)\prod_N^{i=1} C_i^{a_i} \tag{15}$$

257 The parameters used to calculate the reaction rate r, including the pre-exponential factor
258 A and activation energy E, are listed in Table 2.

259 **Table 2.** Coefficient of kinetic parameters

Reaction No.	A (m^3/kmol s)	E (kJ/kmol)
6	4.32e+13	5.55e+4
7	2.38e+17	1.23e+5
8	4.14e+10	3.36e+4
9	7.94e+21	6.59e+4
10	3.62e+10	3.36e+4
11	5.56e+25	7.69e+4

260 Since the absorption reaction is fast and occurs only in the liquid film, the option

261 'Discretize film' is selected for the liquid phase and the number of discrete points is set to be
262 10, and the option 'Consider film' is selected for the gas phase.

263 **3.2 model validation**

264 Model validation is essential to examine the accuracy of the model developed. The
265 experimental cases are obtained from a carbon capture pilot plant campaigns conducted by the
266 University of Texas at Austin. The carbon capture facility used for this campaign was located
267 at the J.J Pickle Research Centre in Austin Texas. In this pilot plant, the diameter and packing
268 height of both absorber and stripper were 0.427m and 6.1m, respectively.

269 The experimental results of this pilot plant have been reported (Plaza, 2011; Plaza and
270 Rochelle, 2011). Platinum resistance temperature detectors were used to measure the gas and
271 liquid phase temperatures at different locations in the absorber. In this study, two independent
272 cases with different L/G ratios were selected to validate the absorber. The selected first and
273 second cases have L/G ratios (mol/mol) of 4.3 and 6.7, respectively, and their temperature
274 measurements are shown in **Fig.9 and 10**. More details on these two cases are shown in **Table**
275 **3**. The temperature profiles of the simulation results corresponding to these cases are shown in
276 **Fig.9 and 10**. Simulation results for these two cases showed capture level of 72.78% and 94.8%,
277 respectively. These results show that the developed model described in section 3.1 is in good
278 agreement with the experimental data.

279 **Table 3.** The operating conditions of selected two absorber cases (Plaza, 2011).

Operating conditions	Case 1 (L/G ratio=4.3)	Case 2 (L/G ratio=6.7)
CO_2 in the flue gas (mol%)	12	12
Flue gas temperature (K)	293	293
PZ concentration (wt%)	40.2	40.3
Lean loading (mol)	0.284	0.267

Gas flowrate (actual m^3/s)	0.165	0.165
Capture level (%)	68.2%	92.2%
Absorber pressure (bar)	1.01	1.01

280

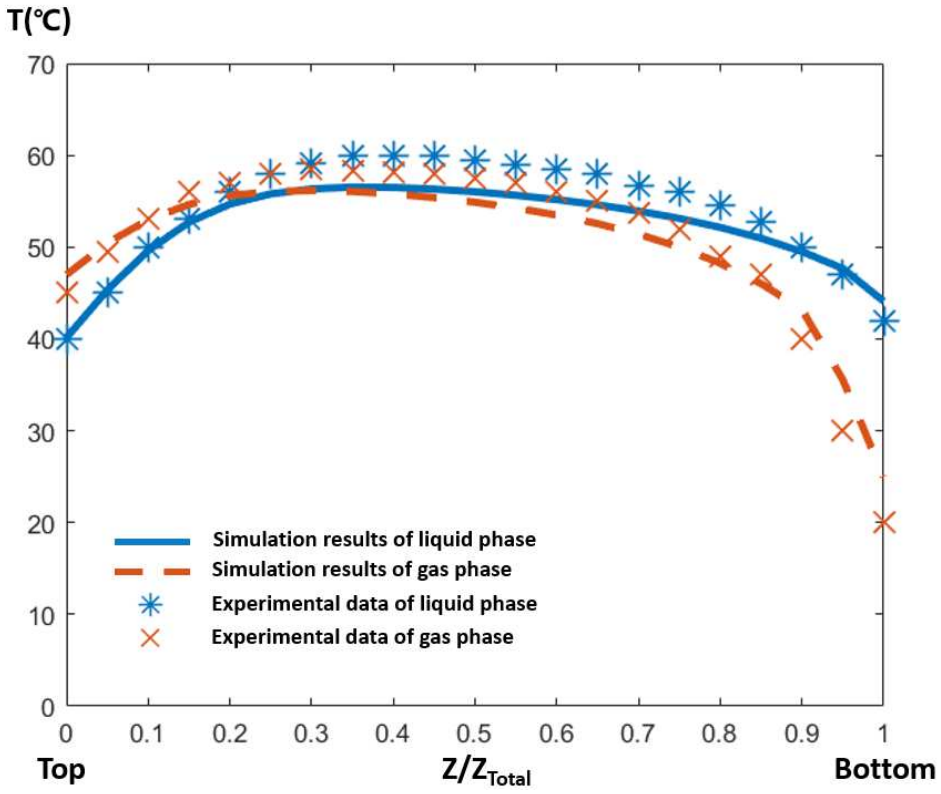

281

282 **Fig.9** Temperature profiles: validation of absorber model at L/G ratio (mol/mol) = 4.3

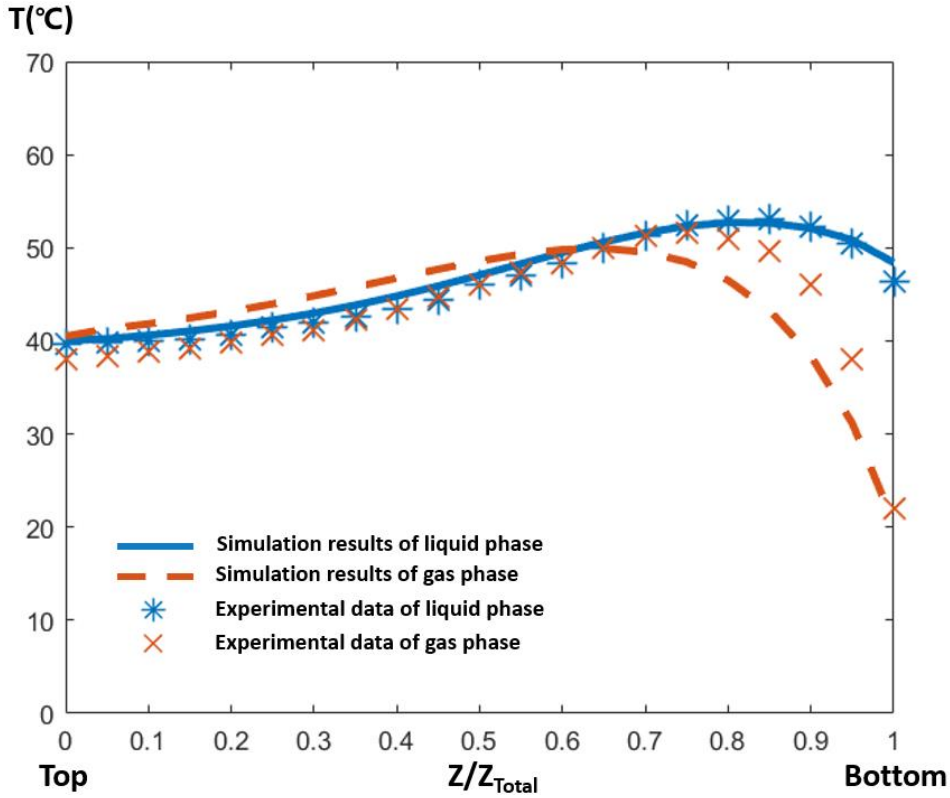

283

Fig.10 Temperature profiles: validation of absorber model at L/G ratio (mol/mol) = 6.7

Experimental data on stripper in this pilot plant program have also been reported (Van Wagener, 2011). The stripper's validation model consists of a cross-heat exchanger, the stripper and the condenser. During the implementation of validation, the flow rate, CO_2 loading and concentration of the rich solvent and reboiler duty were used as the input parameters, and the overhead flow rate and lean loading from the bottom of the stripper were used as the outputs. Operation conditions of stripper cases are summarised in **Table 4**. The comparison of the model predictions and experimental data for reboiler duty is shown in **Fig.11**. The results show that the model correctly predicted the stripper performance and the relative errors are less than 10%.

Table 4. The operating conditions of stripper cases (Van Wagener, 2011).

Operating conditions	Valve
Rich solvent flow (kg/s)	0.85-1.33
PZ concentration (wt%)	28.55-44.15
Stripped CO_2 rate (kg/hr)	39.60-129.60
Rich CO_2 loading (mol_{CO2}/mol_{alk})	0.330-0.404
Condenser temperature (K)	277.95-298.35
Reboiler temperature (K)	360.15-402.15
Stripper pressure (bar)	1.38-4.14
Specific reboiler duty (MJ/kg_{CO2})	3.88-4.59

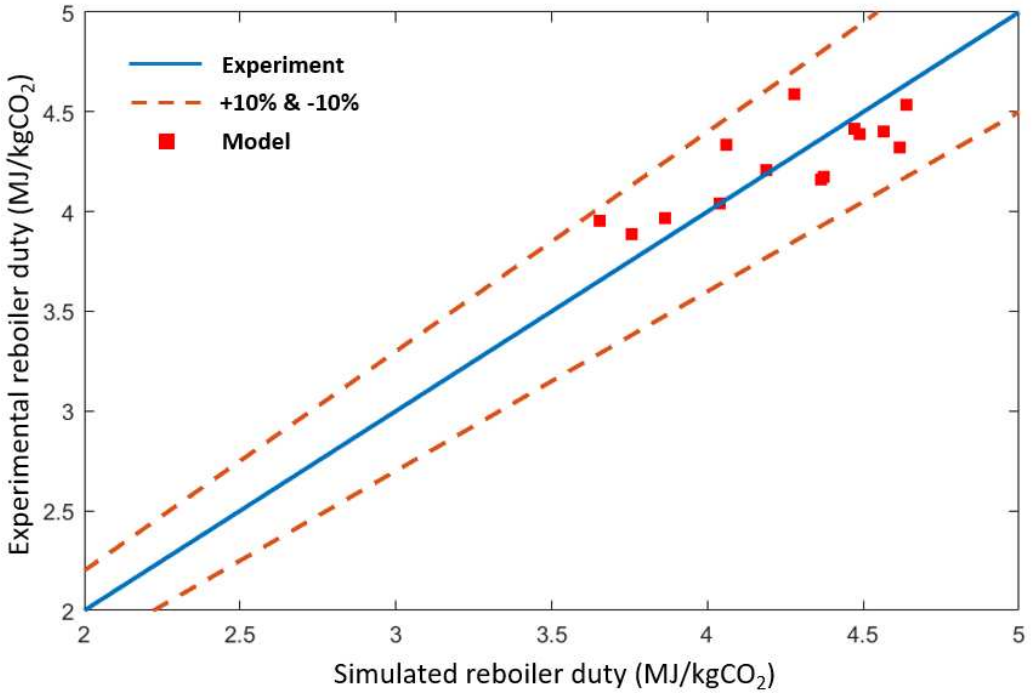

Fig.11 Experimental data versus model prediction for heat duty required for each kilogramme CO_2 regenerated

In summary, the model is in good agreement with the experimental data, and the comparison results show that the proposed modelling method can simulate the absorber and the stripper well.

4. Scale-up of PCC process using PZ for large-scale ethylene plant

The developed PCC model must be scaled up to match the flue gas from 60,000t/year thermal cracking furnace. Before entering the absorber of the PCC process, the flue gas from the thermal cracker has to be cooled to 40°C by either heat exchanger or FHR. The water vapour in flue gas is also cooled to liquid water, which has to be removed. This leads to an increase in the concentration of CO_2 in the flue gas. Moreover, the flue gas at the outlet of the thermal cracking furnace is at a pressure that is slightly less than 1atm. A blower is required to raise the pressure to the absorber pressure. The flue gas flowrate feeding to the absorber is changed to

310 23.27kg/s and its detailed information compared to the flue gas from the thermal cracking

311 furnace is shown in **Table 45**.

312 **Table 45.** The information of the flue gas out of the thermal cracking furnace and into the
313 absorber

Variables	Flue gas out of the thermal cracking furnace	Flue gas into the absorber
Temperature (℃)	115.5	40
Flowrate (kg/s)	24.72	23.27
Pressure (bar)	1.01	1.03
Mole composition		
O_2 (mol%)	3.87	4.25
H_2O (mol%)	15.6	7.22
CO_2 (mol%)	7.69	8.45
N_2 (mol%)	72.84	80.07

314

315 The large-scale capture plant was designed to capture 90% CO_2 in the flue gas using 40

316 wt% PZ solvent. The CO_2 loading in the lean solvent was set to 0.2 mol CO_2/ mol alkalinity.

317 Therefore, the lean solvent mass flowrate to the absorber is estimated using the expression

318 presented as follows:

319 $$L_{Lean} = \frac{G x_{CO_2} \varphi_{CO_2}}{(\alpha_{Rich} - \alpha_{Lean})} \left[\frac{M_{PZ}}{M_{CO_2}} \left(\frac{\omega_{PZ} + 1}{\omega_{PZ}} \right) + \alpha_{Lean} \right] \quad (16)$$

320 The scale-up method that have been proposed (Otitoju et al., 2020) is adopted in this work.

321 This method calculated the diameter of the absorber and stripper based on the flooding velocity

322 using the expressions below:

323 $$V_{G,fl} = \left[\left(\frac{\rho_G}{\rho_L - \rho_G} \right)^{-0.5} \upsilon^{-0.05} {F_P}^{-0.5} \left\{ A \left(\log \left(\frac{L}{G} \sqrt{\frac{\rho_G}{\rho_L}} \right) \right)^2 + B \left(\log \left(\frac{L}{G} \sqrt{\frac{\rho_G}{\rho_L}} \right) \right) + C \right\} \right] \quad (17)$$

324 $$V_G = 0.7 V_{G,fl} \quad (18)$$

325 $$D = \sqrt{\frac{4G}{\pi V_G \rho_G}} \quad (19)$$

Where L and G are solvent mass flowrate (kg/s) and gas mass flowrate (kg/s) respectively, and ρ_L and ρ_G are the density (kg/m^3) of them. It is worth mentioning that the values of density were estimated from pilot plant simulations. The υ is the Kinematic viscosity, which can also be obtained from the simulation results of the pilot plant. The F_P is the packing factor of the Mellapak 2X packing and its value is 205m^{-1}. Where $V_{G,fl}$ stand for flooding velocity, and Eqs.18 means that the column was designed to operate at 70% of the $V_{G,fl}$.

Details of the determination of parameters A, B and C, the calculation of the gas-liquid flowrate for the stripper and the estimation of packing height are available in literature (Otitoju et al., 2020).

Based on the calculation, the estimated dimensions of both absorber and stripper of a large-scale capture plant using PZ solvent for a thermal cracking furnace are presented in **Table ~~5~~6**.

Table ~~5~~6. Estimated dimensions of the absorber and stripper for a 60kt/a ethylene plant.

Items	Estimated results
Absorber	
Diameter(m)	2.8
Packing height(m)	16
Packing type	Mellapak 2X
Stripper	
Diameter(m)	1.6
Packing height(m)	10
Packing type	Mellapak 2X

5. Case studies of different configurations of the PCC process using PZ for ethylene plants

In this section, four case studies that adopted various configurations of the PCC model described in Section 2 are designed and simulated in Aspen Plus®. In section 5.1, the standard PCC process using PZ solvent for a 60,000 t/year ethylene plant is simulated and optimized.

The coupling of the proposed FHR and the standard configuration is designed in Section 5.2. The intercooled configuration with FHR is studied in Section 5.3. In Section 5.4, the process configuration consisting of AFS, absorber inter-cooling and FHR is designed and simulated to study the potential of energy consumption reduction in the PCC process using PZ solvent for an ethylene plant.

5.1 Case 1: standard PCC process

The flue gas composition changes as it leaves the thermal cracking furnace and enters the absorber. This is due to pressurization and cooling. the simulation results of the flue gas have been shown in **Table 45**.

The closed-loop model of the PCC process is developed using the estimated dimensions of the absorber and stripper shown in **Fig.12**. Other input parameters of the standard PCC process are listed in **Table 67**. From the simulation results, the solvent regeneration energy consumption is 2.82 GJ/tCO_2 when PZ-based standard PCC is used without FHR.

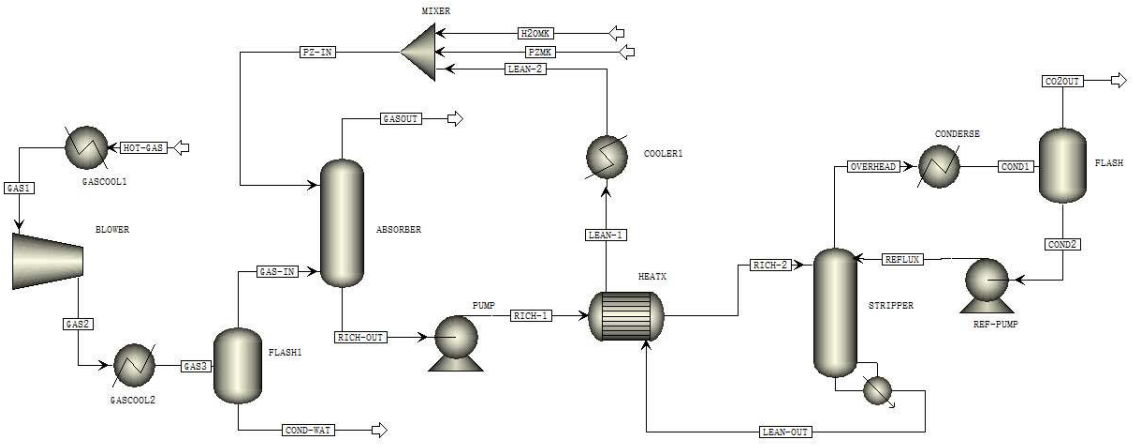

Fig.12 The topology of standard configuration

Table 67. Process input parameter of standard PCC process

Parameters	Values
CO_2 capture level	90%

Lean solvent flowrate (kg/s)	40.2
PZ concentration (wt%)	40
Lean solvent temperature (K)	312
Rich solvent pump pressure (bar)	2
Cross heat exchanger temperature approach (K)	10
Absorber pressure (bar)	1.01
Stripper pressure (bar)	1.65
Condenser temperature (K)	308.15

5.2 Case 2: Standard PCC process with proposed FHR

The sum of the cooler duty of the flue gas in the standard configuration of the PCC process is 5.66MW, which means that there is substantial heat in the flue gas. However, the maximum flue gas temperature of 115.5℃ is not suitable for heating the reboiler, which requires a heat source above 123℃. The flue gas heat is used to heat a portion of the rich solvent before entering the absorber. The rich solvent is divided into two portions. A portion of this stream is sent to a heat exchanger where its temperature is raised to about 100℃. Another portion of the rich solvent is sent through the cross-heat exchanger. These solvents are combined before entering the stripper. The topology of the standard configuration with FHR is shown in **Fig.13**. The rest of the operating conditions and input parameters are similar to the standard process.

The simulation results of rich solvent temperature in different streams are shown in **Fig.14**. It can be seen that the temperature of the rich solvent entering the stripper can be increased by FHR, thus increasing the potential for a reduction in the regeneration energy consumption.

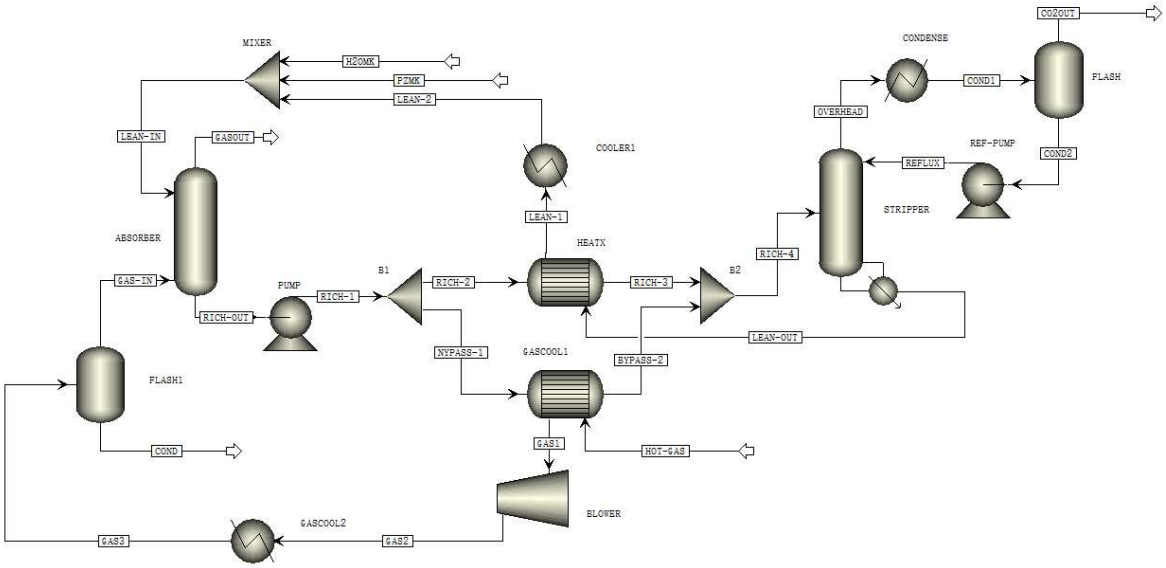

373

374 **Fig. 13** The topology of standard configuration with FHR

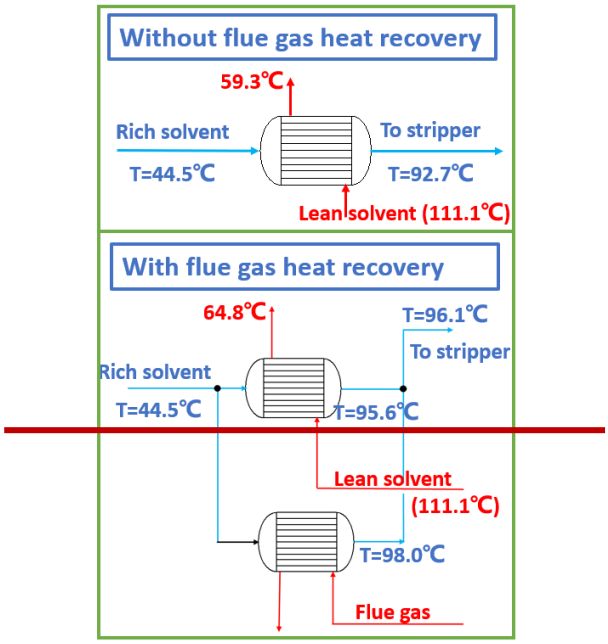

375

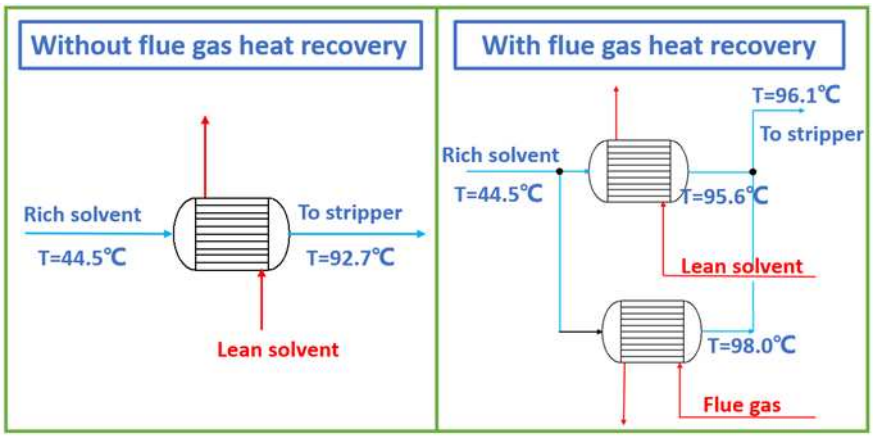

376

Fig. 14 Rich solvent temperatures with and without FHR

Due to the volume fraction of water in the flue gas from the thermal cracking furnace being 15.6mol%, the dew point is at around 60℃, hence the heat that can be recovered from the flue gas is limited. The simulation results show that the recovered heat duty is 1.37MW (heat duty of GASCOOL1 in **Fig.13**), and the reboiler duty is reduced by 0.38MW. The reason for this gap is that the introduction of FHR leads to a reduction in the heat recovery of the lean solvent. The lean solvent temperature in the different streams is shown in **Fig.14.** From the simulation results, the solvent regeneration energy consumption is 2.60 GJ/tCO_2 when PZ-based standard PCC is used with FHR.

5.3 Case 3: configuration of Absorber inter-cooling with FHR

The absorber inter-cooling is simulated using two connected absorber sections (i.e. RadFrac in Aspen Plus®), an absorber intercooler and an intercooler pump is shown in **Fig 15**. Inter-cooling improves the absorption capacity of lean solvent, which leads to a reduction of solvent requirement and packing height in the absorber. The dimensions of the absorber and solvent flowrate with and without absorber inter-cooling are shown in **Table ~~7~~8**.

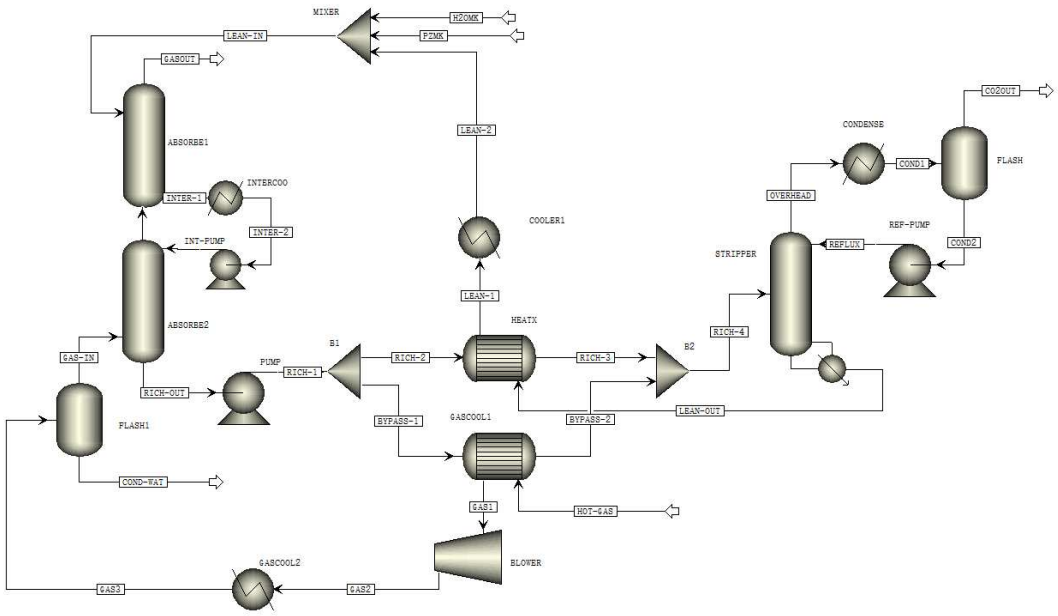

Fig. 15 The topology of absorber inter-cooling with FHR

Table ~~7~~8. Parameters with and without absorber inter-cooling

Items	Standard configuration	Standard configuration with absorber inter-cooling
Absorber diameter (m)	2.8	2.6
Absorber packing height (m)	16	12
Solvent flowrate (kg/s)	40.2	37.45

In the optimal position of the inter-cooling, the solvent flowrate is 37.45 kg/s which is 6.8% less than that in the standard process due to better chemical absorption. In addition, the configuration of inter-cooling only (without FHR) was also simulated for comparison. The simulation results indicate that the reduction in energy consumption contributed by FHR in the standard and absorber inter-cooling configuration is 0.142 GJ/tCO_2 and 0.180 GJ/tCO_2, respectively. This is due to the lower temperature of the rich solvent from the absorber increasing the recovered heat in the flue gas. From this, it can be seen that the FHR and absorber inter-cooling have a better-coordinated effect. The reboiler duty of absorber inter-cooling configuration with FHR is further reduced by 0.48MW compared to Case 2. From the

simulation results, the solvent regeneration energy consumption reduces to 2.47 GJ/tCO_2 when PZ-based PCC is used with FHR and inter-cooling.

5.4 Case 4: AFS configuration with absorber inter-cooling and FHR

In this case study, the configuration combining the AFS, absorber inter-cooling and FHR is designed and simulated to explore the energy-saving potential. The last stage of the stripper is designated as the reboiler, which was simulated using a steam heater and a flash tank. The topology of configuration including AFS, absorber inter-cooling and FHR is shown in **Fig.16**.

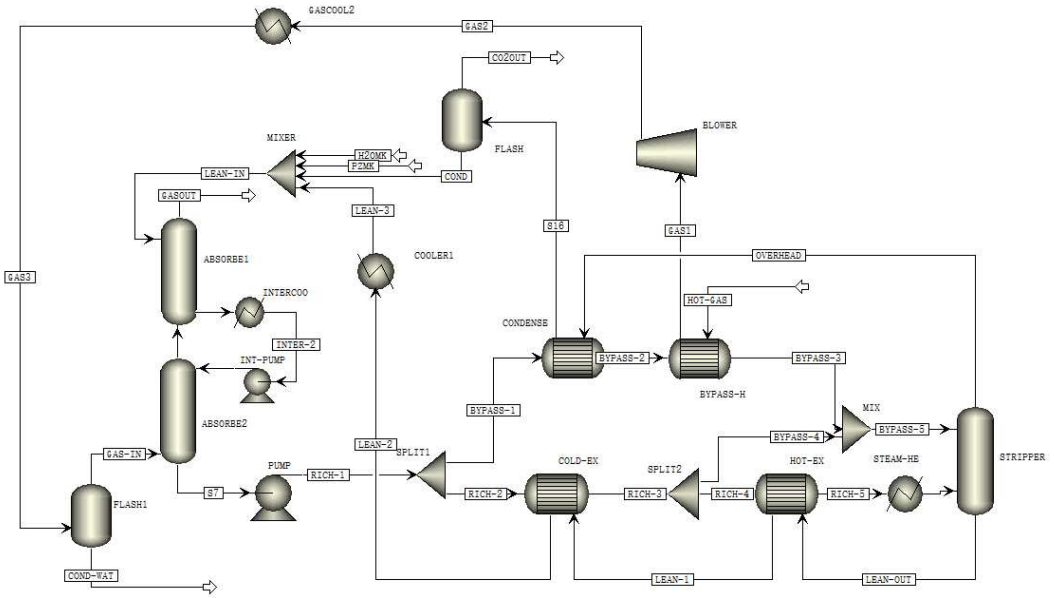

Fig. 16 The topology of AFS configuration with absorber inter-cooling and FHR

The heat recovery capacity of rich solvent from the bottom of the absorber was studied to design and optimize the AFS configuration. The temperature-enthalpy diagram for heating the rich solvent shown in **Fig.17** indicates that the temperature change in the low-temperature section is higher than in the high-temperature section for the same heat supply.

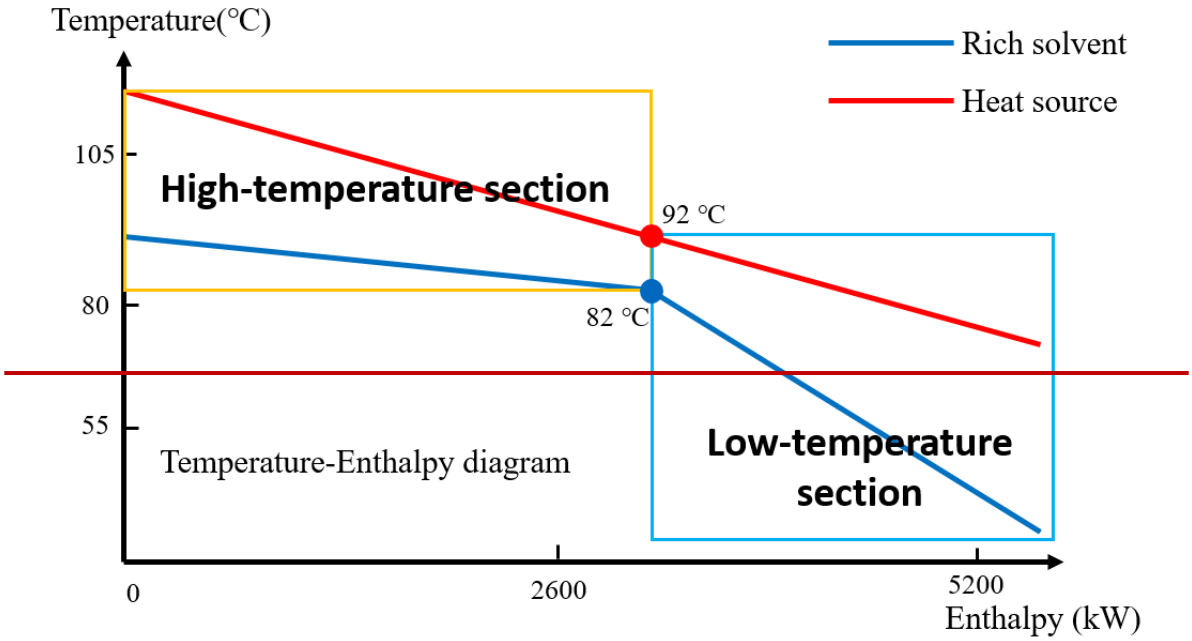

418

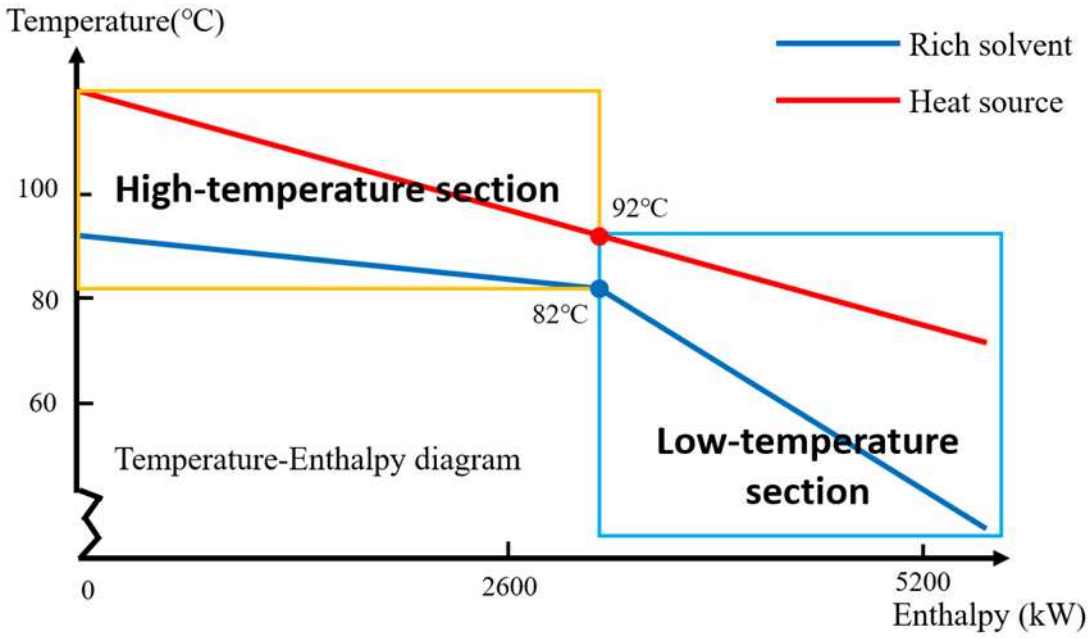

419

420 **Fig.17** Temperature-enthalpy diagram for heating the rich solvent

421 This phenomenon leads to the simulated results that the heat requirement of rich solvent

422 in the low-temperature section is easily satisfied by the heat recovery from flue gas and lean

423 solvent. In the AFS configuration, the heat of the saturated water vapour at the top of the stripper

424 is recovered, but its temperature is relatively low, in the Low-temperature section, and can only

425 heat the rich solvent to about 90°C, whereas the flue gas heated the rich liquid to 97.4°C thus

saving even more energy.

The AFS configuration improves the heat exchanger duty in high-temperature sections by distributing the stream exchanged with lean solvent. Therefore, the drawback of FHR described in Section 5.2 (i.e. reduction in heat recovery of lean solvent) is overcome. From the simulation results, the solvent regeneration energy consumption reduces to 2.28 GJ/tCO_2 when PZ-based PCC (including AFS and inter-cooling) is used with FHR.

6. Technical and economic assessment

6.1 Technical assessment

The energy performance of different configurations of the carbon capture process using 40 wt% PZ is assessed based on energy consumption for rich solvent regeneration in the stripper, duty of coolers used to cool the flue gas and the electricity consumption for pumps and the blower. This represents the total energy consumption in the capture process. The captured CO_2 from the stripper is compressed using a multistage compressor process simulated in Aspen Plus®. In the simulation, the compression efficiency was set as 72%. The electricity consumption for compression is ~~646.9~~1139.5kW in all four cases. The carbon capture process using 30 wt% MEA for the ethylene plant (Hu et al., 2023) was considered as a baseline for comparison with different configurations using 40 wt% PZ in this study. The energy performance of the four cases is summarised in **Table ~~8~~9**.

444 **Table 89.** Energy performance of the PCC process with different configurations.

Description	Standard configuration using 30 wt% MEA (Hu et al., 2023)	Case 1: standard configuration using 40 wt% PZ	Case 2: standard configuration with FHR using 40 wt% PZ	Case 3: configuration of absorber inter-cooling with FHR using 40 wt% PZ	Case 4: configuration consists of AFS, absorber inter-cooling and FHR using 40 wt% PZ
Duty of coolers (MW)	11.29	9.68	9.31	9.86	9.28
Duty of coolers (GJ/CO_2)	4.17	3.57	3.44	3.64	3.20
Electricity consumption in carbon capture process(kW)	118.14	82.20	83.43	83.17	89.98
Electricity consumption in compression process(kW)	1139.5	1139.5	1139.5	1139.5	1139.5
Reboiler heat duty (MW)	9.92	7.52	7.14	6.79	6.25
Reboiler regeneration consumption (GJ/tonCO_2)	3.66	2.82	2.60	2.47	2.28

445

446 The 115.5℃ flue gas from the ethylene cracking furnace needs to be cooled down. When
447 the configuration of FHR is adopted, the amount of cooling energy consumption required is
448 reduced. Case 3 requires slightly more cooling consumption than Case 2 due to the additional
449 cooling requirements of the absorber intercooler. In addition, Cases 2 to 4 (with FHR) consume
450 more electricity than Case 1 (without FHR), which is caused by different gas inlet pressure of
451 the blower.

452 It can be seen that Case 4 (AFS plus inter-cooling configuration with FHR using 40 wt%
453 PZ) has the lowest regeneration energy consumption, with a 37.71% reduction compared to the
454 baseline (standard configuration using 30 wt% MEA as reported in Hu et al. 2023). Such a
455 significant reduction in energy consumption is caused by the change of solvent (from 30 wt%
456 MEA to 40 wt% PZ), FHR and configuration improvements (with AFS and inter-cooling).

457 Comparison between Case 1 (the standard configuration using 40 wt% PZ) and the
458 baseline (standard configuration using 30 wt% MEA as reported in Hu et al. 2023) shows that
459 replacing the solvent reduces energy consumption by 22.95%. With the addition of FHR (in
460 Case 2), the energy consumption reduction is 28.96% compared with baseline. This indicates
461 the net contribution from FHR is 6.01%. With additional configuration improvements
462 (including AFS and inter-cooling) as shown in Case 4, the energy consumption reduction is
463 37.71% compared with baseline. This indicates the net contribution from configuration
464 improvement is 8.75%.

465 **6.2 Economic assessment**

466 Different configurations of the PCC process for ethylene plants in Cases 1-4 are assessed
467 using Aspen Economic Process Analyzer® (APEA) to understand their economic potential. In
468 APEA, equipment size is estimated according to process conditions, and then the equipment
469 cost and total direct cost (TDC) are evaluated.

470 The cost of the plant consists of capital expenditure (CAPEX) and operation expenditure
471 (OPEX). In APEA, the TDC of the equipment (e.g. absorber, stripper, pumps, heat exchangers)
472 in different configurations of the PCC processes is estimated. The direct equipment costs and
473 the calculated CAPEX for the four cases and the benchmark process with 30 wt% MEA are

provided in **Table ~~9~~10** and **Table ~~10~~11**, respectively.

Table 910. Total direct cost of the different configurations of the PCC plant for the ethylene plant.

Equipment	Standard Process +30 wt% MEA (Hu et al., 2023)	Case1: Standard Process +40 wt% PZ	Case2: Standard Process +FHR +40 wt% PZ	Case3: Absorber inter-cooling +FHR +40 wt% PZ	Case4: Absorber inter-cooling +Advance flash stripper +FHR +40 wt% PZ
	Direct cost (M$)	Direct cost (M$)	Direct cost (M$)	Direct cost (M$)	Direct cost (M$)
Absorber	2.128	0.927	0.927	0.682	0.682
Solvent storage vessel	0.030	0.020	0.020	0.020	0.020
Rich pump	0.066	0.064	0.064	0.064	0.064
Flash		0.214	0.214	0.214	0.214
Condenser	0.105	0.105	0.108	0.105	0.143
Stripper reflux drum	0.089	0.104	0.104	0.104	
Stripper reboiler	0.179	0.154	0.151	0.149	
Stripper reflux pump	0.034	0.035	0.035	0.035	
Stripper	0.610	0.334	0.334	0.334	0.334
Lean cooler	0.081	0.122	0.125	0.122	0.128
Main cross-heat exchanger	0.209	0.214	0.205	0.202	
Intercooler				0.122	0.122
Intercooler pump				0.070	0.070
Cold exchanger					0.170
Hot exchanger					0.177
Steam heater					0.136
Flash tank					0.109
Blower	0.049	0.049	0.049	0.049	0.049
Flue gas coolers	0.302	0.302	0.135	0.135	0.131
FHR exchanger			0.131	0.131	0.107
Total Direct Cost (TDC)	3.883	2.643	2.603	2.538	2.657

Table ~~10~~11. CAPEX of the different configurations of the PCC plant for the ethylene plant.

Description (M$)	Standard Process +30 wt% MEA (Hu et al., 2023)	Case1: Standard Process +40 wt% PZ	Case2: Standard Process +FHR +40 wt% PZ	Case3: Absorber inter-cooling +FHR +40 wt% PZ	Case4: Absorber inter-cooling +Advance flash stripper +FHR +40 wt% PZ
Total direct cost (TDC)	3.883	2.643	2.603	2.538	2.657
Total indirect cost (TIC) =20% of TDC	0.777	0.529	0.521	0.508	0.531
Bare erected cost (BEC) =TDC+TIC	4.660	3.172	3.123	3.046	3.188
Engineering and Contractor (EC) =27% of BEC	1.258	0.856	0.843	0.822	0.861
Engineering procurement and construction (EPC) =127% of BEC	5.918	4.028	3.967	3.868	4.049
Process contingency (PC) =25% of BEC	1.165	0.793	0.781	0.761	0.797
Project contingency (PJC) =20% of EPC + 5% of BEC	1.417	0.964	0.950	0.926	0.969
Total plant cost (TPC) =120% of EPC +30% of BEC	8.499	5.785	5.697	5.556	5.815
Owner's cost (OC) =15% of TPC	1.275	0.868	0.855	0.833	0.872
Total capital expenditure (CAPEX) =115% of TPC	9.774	6.653	6.552	6.389	6.687

The total annual cost consists of the annual capital cost (ACC) and annual operating costs. The ACC can be calculated by Eq.20. In this equation, n is the project life and i is the interest rate. The life cycle of the plant is assumed as 20 years and the interest rate is assumed as 10%.

$$ACC = \frac{CAPEX}{\frac{(1+i)^n - 1}{i(1+i)^n}} \quad (20)$$

OPEX consists of fixed operating and maintenance (fixed O&M) costs and variable operating and maintenance (variable O&M) costs. The fixed O&M cost includes maintenance costs, labour costs etc. and is assumed as 3% of the CAPEX (Luo et al., 2016). The variable O&M cost mainly contains supplementary solvent costs and the utility costs. Prices of the utilities such as steam, cooling water and electricity are from East China. The unit prices of process utilities are listed in **Table ~~11~~12**. Hu et al. (2023) compared the heat integration of a gasoline fractionator to the PCC process with the standard PCC process in East China, but the price of low-pressure steam was much lower than the actual price and the equipment cost of the blower was grossly overestimated, so the results and the savings in operating costs are not practical. We performed an economic assessment for the standard PCC process using 30 wt% MEA. The amount of solvent added is calculated by solvent degradation, which is assumed as 1.5kg/tonCO_2 and 0.05kg/tonCO_2 for MEA and PZ (Knudsen et al., 2009), respectively. Unit prices of amine solvents are listed in **Table ~~11~~12**. It is worth mentioning that due to the high moisture content of the flue gas from the ethylene-cracking furnace, a flash separator is used to discharge the condensed water from the cooled flue gas. The amount of the condensed water is larger than the evaporated water in the absorber, so no additional water makeup is required for the PCC plant in all the configurations.

Table ~~11~~12. Unit prices of utilities and amine solvents.

Description	Unit price[b]
Cooling water ($/MJ)	0.0002
Electricity ($/kWh)	0.103
Mid-pressure steam ($/MJ)	0.0143
Make-up MEA ($/ton)[a]	1,295
Make-up PZ ($/ton)[a]	5,750

[a] Prices obtained from b2b.baidu.com.
[b]The exchange rate between CNY and USD is 6.95 yuan/dollar in March 2023.

The operating time is 8,000 hours per year. The annual total costs and CO_2 capture costs are

505 listed in **Table ~~12~~13**. The above tables do not include the cost to compress the captured CO_2
506 from stripper pressure to 150 bar. Three-stage compression is used for CO_2 compression. The
507 total direct cost of the compressors is 3.44M$, and the electricity consumption is 1139.5kW.
508 The annual total cost and CO_2 capture cost with compression are produced in **Table ~~13~~14**.

Table ~~12~~13. Summary of the economic performance of PCC plant with different configurations.

Description		Standard Process +30 wt% MEA (Hu et al., 2023)	Standard Process +40 wt% PZ	Standard Process +FHR +40 wt% PZ	Absorber inter-cooling +FHR +40 wt% PZ	Absorber inter-cooling +Advance flash stripper +FHR +40 wt% PZ
ACC (M$/year)		1.148	0.781	0.770	0.750	0.785
Fixed O&M cost (M$/year)		0.293	0.200	0.197	0.192	0.201
variable O&M cost	Electricity (M$/year)	0.073	0.051	0.052	0.052	0.056
	Cooling water (M$/year)	0.069	0.059	0.057	0.060	0.057
	Mid-pressure steam (M$/year)	4.069	3.086	2.931	2.787	2.565
	Make-up solvent ($/year)	0.151	0.022	0.022	0.022	0.022
Total capture cost (M$/year)		5.828	4.200	4.029	3.864	3.686
CO_2 capture cost ($/ton$CO_2$)		74.75	53.87	51.67	49.55	47.27

Table ~~13~~14. Comparison of CO_2 capture cost of PCC processes with compression and without compression.

Description		Standard Process +30 wt% MEA (Hu et al., 2023)	Standard Process +40 wt% PZ	Standard Process +FHR +40 wt% PZ	Absorber inter-cooling +FHR +40 wt% PZ	Absorber inter-cooling +Advance flash stripper +FHR +40 wt% PZ
TDC	without compressors (M$)	3.883	2.643	2.603	2.538	2.657
	including compressors (M$)	7.323	6.083	6.043	5.978	6.097
CO_2 capture cost	without compression ($/ton$CO_2$)	74.75	53.87	51.67	49.55	47.27
	including compression ($/ton$CO_2$)	100.19	79.31	77.12	74.99	72.71

For the baseline (standard configuration using 30 wt% MEA as reported in Hu et al. 2023), its carbon capture cost is 74.75 \$/tonCO_2. The capture cost for Case 1 (the standard configuration using 40 wt% PZ) reduces to 53.87 \$/tonCO_2. This means a cost reduction by 27.93% due to the change of solvent. The capture cost for Case 2 (PZ-based standard configuration with FHR) is 51.67 \$/tonCO_2. This means a cost reduction by 30.87%. The net contribution on cost reduction due to FHR is 2.94%. The lowest carbon capture cost of 47.27 \$/tonCO_2 was achieved in Case 4 (PZ-based PCC with FHR, inter-cooling and AFS), a reduction of 36.76% against the baseline. The net contribution from configuration improvement (i.e. AFS and inter-cooling) on capture cost reduction is 5.89%.

7. Conclusions

An FHR strategy involving heat exchange with rich solvent is proposed and designed through thermodynamic analysis of the carbon capture process. In order to reduce the capture cost and energy consumption, a rate-based model for PCC using PZ was developed in Aspen Plus®, model validation with pilot plant data and scale-up for 60,000t/year ethylene plant. The standard configuration using 30 wt% MEA is viewed as baseline. Four cases using 40 wt% PZ were studied and techno-economically evaluated. The technical evaluation results show an energy consumption reduction of 37.71% against the baseline. The change of solvent (from 30 wt% MEA to 40 wt% PZ) has the highest contribution to the reduction of energy consumption of 22.95%, followed by contribution from configuration improvement of 8.75% and contribution from FHR of 6.01%. The economic analysis indicates that Case 4 has the lowest carbon capture cost of 47.27 \$/tonCO_2, a 36.76% reduction compared to the baseline. The

implementation of the PZ-based PCC process with FHR, inter-cooling and AFS can significantly reduce the carbon capture cost and energy consumption of PCC process for large-scale ethylene plants.

CRediT authorship contribution statement

Jin Ma: Conceptualization, Methodology, Validation, Investigation, Visualization, Writing - original draft. **Zhaoxi Dong:** Investigation, Formal analysis. **Olajide Otitoju:** Writing - review & editing. **Meihong Wang:** Supervision, Writing - review & editing. **Wenli Du:** Resources. **Feng Qian:** Supervision.

Declaration of Competing Interest

The authors declare that they have no known competing financial interests or personal relationships that could have appeared to influence the work reported in this paper.

Acknowledgements

This work is supported by the National Key Research & Development Program - Intergovernmental International Science and Technology Innovation Cooperation Project (2021YFE0112800). The UK authors would like to acknowledge the financial support of the EU RISE project OPTIMAL (Ref 101007963).

References：

Akinpelumi, K., Saha, C., & Rochelle, G. T. (2019). Piperazine aerosol mitigation for post-combustion carbon capture. *International Journal of Greenhouse Gas Control*, *91*. https://doi.org/10.1016/j.ijggc.2019.102845

Alabdulkarem, A., Hwang, Y., & Radermacher, R. (2015). Multi-functional heat pump integration in power plants for CO_2 capture and sequestration. *Applied Energy*, *147*, 258–268. https://doi.org/10.1016/j.apenergy.2015.03.003

Arshad, M., Wukovits, W., & Friedl, A. (2014). Simulation of CO_2 absorption using the system K2CO3-Piperazine. *Chemical Engineering Transactions*, *39*(Special Issue), 577–582. https://doi.org/10.3303/CET1439097

Aspen Tech. Aspen Physical Properties System - Physical Property Methods. available online. http://support.aspentech.com/ (accessed August 20, 2020).

Biliyok, C., Lawal, A., Wang, M., & Seibert, F. (2012). Dynamic modelling, validation and analysis of post-combustion chemical absorption CO_2 capture plant. *International Journal of Greenhouse Gas Control*, *9*, 428–445. https://doi.org/10.1016/j.ijggc.2012.05.001

Canepa, R., Wang, M., Biliyok, C., & Satta, A. (2013). Thermodynamic analysis of combined cycle gas turbine power plant with post-combustion CO_2 capture and exhaust gas recirculation. *Proceedings of the Institution of Mechanical Engineers, Part E: Journal of Process Mechanical Engineering*, *227*(2), 89–105. https://doi.org/10.1177/0954408912469165

Chen, E., Zhang, Y., Lin, Y., Nielsenb, P., & Rochelle, G. (2017). Review of Recent Pilot Plant Activities with Concentrated Piperazine. *Energy Procedia*, *114*, 1110–1127. https://doi.org/10.1016/j.egypro.2017.03.1266

Chen, M., Luo, Q., Lin, H., Sun, Q., Gao, H., Liu, S., Li, Y., & Liang, Z. (2023). A study on reaction mechanism and kinetics of CO_2 and MEA/DEA-tertiary amines in non-aqueous and water-lean solutions. *Chemical Engineering Science*, *269*. https://doi.org/10.1016/j.ces.2022.118431

China Chemical Industrial Mechanism Power Technology Association, 2021. Economic operation forecast of China's petroleum and chemical industry. http://www.ccimp.org/aspcms/news/2021-2-22/297.html.

Cullinane, J. T., & Rochelle, G. T. (2006). Kinetics of carbon dioxide absorption into aqueous potassium carbonate and piperazine. *Industrial and Engineering Chemistry Research*, *45*(8), 2531–2545. https://doi.org/10.1021/ie050230s

Dugas, R. E., & Rochelle, G. T. (2011). CO_2 absorption rate into concentrated aqueous monoethanolamine and piperazine. *Journal of Chemical and Engineering Data*, *56*(5), 2187–2195. https://doi.org/10.1021/je101234t

Dugas, R., & Rochelle, G. (2009). Absorption and desorption rates of carbon dioxide with monoethanolamine and piperazine. *Energy Procedia*, *1*(1), 1163–1169. https://doi.org/10.1016/j.egypro.2009.01.153

Ermatchkov, V., Pérez-Salado Kamps, Á., & Maurer, G. (2003). Chemical equilibrium constants for the formation of carbamates in (carbon dioxide + piperazine + water) from 1H-NMR-spectroscopy. *Journal of Chemical Thermodynamics*, *35*(8), 1277–1289. https://doi.org/10.1016/S0021-9614(03)00076-4

Frailie DH. Modeling of Carbon Dioxide Absorption/Stripping by Aqueous Methyldiethanolamine/Piperazine. PhD Thesis, USA: University of Texas at Austin; 2014.

Frailie, P., Plaza, J., van Wagener, D., & Rochelle, G. T. (2011). Modeling piperazine thermodynamics. *Energy Procedia*, *4*, 35–42. https://doi.org/10.1016/j.egypro.2011.01.020

Freeman, S. A., Davis, J., & Rochelle, G. T. (2010). Degradation of aqueous piperazine in carbon dioxide capture. *International Journal of Greenhouse Gas Control*, *4*(5), 756–761. https://doi.org/10.1016/j.ijggc.2010.03.009

Freeman, S. A., Dugas, R., van Wagener, D. H., Nguyen, T., & Rochelle, G. T. (2010). Carbon dioxide capture with concentrated, aqueous piperazine. *International Journal of Greenhouse Gas Control*, *4*(2), 119–124. https://doi.org/10.1016/j.ijggc.2009.10.008

Gabrielli, P., Rosa, L., Gazzani, M., Meys, R., Bardow, A., Mazzotti, M., & Sansavini, G. (2023). Net-zero emissions chemical industry in a world of limited resources. In One Earth (Vol. 6, Issue 6, pp. 682–704). Cell Press. https://doi.org/10.1016/j.oneear.2023.05.006

Gao DH. Absorber Modeling and Design in Amine Scrubbing for Carbon Capture. PhD Thesis, USA: University of Texas at Austin; 2021.

Gao, T., & Rochelle, G. T. (2020). CO_2 Absorption from Gas Turbine Flue Gas by Aqueous Piperazine with Intercooling. *Industrial and Engineering Chemistry Research*, *59*(15), 7174–7181. https://doi.org/10.1021/acs.iecr.9b05733

Gao, T., & Rochelle, G. T. (2022). Creative absorber design and optimization for CO_2 capture with aqueous piperazine. *International Journal of Greenhouse Gas Control*, *113*. https://doi.org/10.1016/j.ijggc.2021.103534

Hetzer, H. B., Robinson, R. A., & Bates, R. G. (n.d.). *Dissociation Constants of Piperazinium Ion and Related Thermodynamic Quantities from 0 to 50°*. https://pubs.acs.org/sharingguidelines

Horvath AL. Handbook of aqueous electrolyte solutions: Physical properties, estimation and correlation methods. Chichester: Ellis Horwood; 1985.

Hu, G., Li, X., Liu, X., Hu, J., Otitoju, O., Wang, M., Du, W., Ye, Z., Long, J., & Qian, F. (2023). Techno-economic evaluation of post-combustion carbon capture based on chemical absorption for the thermal cracking furnace in ethylene manufacturing. *Fuel*, *331*. https://doi.org/10.1016/j.fuel.2022.125604

Jin, H., Liu, P., & Li, Z. (2021). Impact of solvent properties on post-combustion carbon capture processes: A vapor–liquid equilibrium modelling approach. *Chemical Engineering Science: X*, *10*. https://doi.org/10.1016/j.cesx.2021.100095

Keller, F., Lee, R. P., & Meyer, B. (2020). Life cycle assessment of global warming potential, resource depletion and acidification potential of fossil, renewable and secondary feedstock for olefin production in Germany. *Journal of Cleaner Production*, *250*. https://doi.org/10.1016/j.jclepro.2019.119484

Kim, I., & Svendsen, H. F. (2007). Heat of absorption of carbon dioxide (CO_2) in monoethanolamine (MEA) and 2-(aminoethyl)ethanolamine (AEEA) solutions. *Industrial and Engineering Chemistry Research*, *46*(17), 5803–5809. https://doi.org/10.1021/ie0616489

Lawal, A., Wang, M., Stephenson, P., & Obi, O. (2012). Demonstrating full-scale post-combustion CO 2 capture for coal-fired power plants through dynamic modelling and simulation. *Fuel*, *101*, 115–128. https://doi.org/10.1016/j.fuel.2010.10.056

Lawal, A., Wang, M., Stephenson, P., Koumpouras, G., & Yeung, H. (2010). Dynamic modelling and analysis of post-combustion CO_2 chemical absorption process for coal-fired power plants. *Fuel*, *89*(10), 2791–2801. https://doi.org/10.1016/j.fuel.2010.05.030

Li, H., Frailie, P. T., Rochelle, G. T., & Chen, J. (2014). Thermodynamic modeling of piperazine/2-aminomethylpropanol/CO_2/water. *Chemical Engineering Science*, *117*, 331–341. https://doi.org/10.1016/j.ces.2014.06.026

Li, L., Voice, A. K., Li, H., Namjoshi, O., Nguyen, T., Du, Y., & Rochelle, G. T. (2013). Amine blends using concentrated piperazine. *Energy Procedia*, *37*, 353–369. https://doi.org/10.1016/j.egypro.2013.05.121

Lin, Y. J., Chen, E., & Rochelle, G. T. (2016). Pilot plant test of the advanced flash stripper for CO_2 capture. In *Faraday Discussions* (Vol. 192, pp. 37–58). Royal Society of Chemistry. https://doi.org/10.1039/c6fd00029k

Liu, C. T., Fischer, K. B., & Rochelle, G. T. (2020). Corrosion by Aqueous Piperazine at 40-150 °c in Pilot Testing of CO_2 Capture. *Industrial and Engineering Chemistry Research*, *59*(15), 7189–7197. https://doi.org/10.1021/acs.iecr.9b05735

Luo, Q., Sun, Q., Liu, Q., Liu, S., Xiao, M., Chen, M., Li, Y., Gao, H., & Liang, Z. (2022). Kinetics of CO_2 absorption into ethanolamine + water + ethanol system—mechanism, role of water, and kinetic model. *Chemical Engineering Science*, *259*. https://doi.org/10.1016/j.ces.2022.117732

Mangalapally, H. P., & Hasse, H. (2011). Pilot plant study of two new solvents for post combustion carbon dioxide capture by reactive absorption and comparison to monoethanolamine. *Chemical Engineering Science*, *66*(22), 5512–5522. https://doi.org/10.1016/j.ces.2011.06.054

Mynko, O., Amghizar, I., Brown, D. J., Chen, L., Marin, G. B., de Alvarenga, R. F., Uslu, D. C., Dewulf, J., & van Geem, K. M. (2022). Reducing CO_2 emissions of existing ethylene plants: Evaluation of different revamp strategies to reduce global CO_2 emission by 100 million tonnes. *Journal of Cleaner Production*, *362*. https://doi.org/10.1016/j.jclepro.2022.132127

Na, S., Hwang, S. J., Kim, H., Baek, I. H., & Lee, K. S. (2019). Modeling of CO_2 solubility of an aqueous polyamine solvent for CO_2 capture. *Chemical Engineering Science*, *204*, 140–150. https://doi.org/10.1016/j.ces.2019.04.021

Nguyen, T., Hilliard, M., & Rochelle, G. T. (2010). Amine volatility in CO_2 capture. *International Journal of Greenhouse Gas Control*, *4*(5), 707–715. https://doi.org/10.1016/j.ijggc.2010.06.003

Nwaoha, C., Idem, R., Supap, T., Saiwan, C., Tontiwachwuthikul, P., Rongwong, W., Al-Marri, M. J., & Benamor, A. (2017). Heat duty, heat of absorption, sensible heat and heat of vaporization of 2–Amino–2–Methyl–1–Propanol (AMP), Piperazine (PZ) and Monoethanolamine (MEA) tri–solvent blend for carbon dioxide (CO_2) capture. *Chemical Engineering Science*, *170*, 26–35. https://doi.org/10.1016/j.ces.2017.03.025

Otitoju, O., Oko, E., & Wang, M. (2020). A new method for scale-up of solvent-based post-combustion carbon capture process with packed columns. *International Journal of Greenhouse Gas Control*, *93*. https://doi.org/10.1016/j.ijggc.2019.102900

Otitoju, O., Oko, E., & Wang, M. (2021). Technical and economic performance assessment of post-combustion carbon capture using piperazine for large scale natural gas combined cycle power plants through process simulation. *Applied Energy*, *292*. https://doi.org/10.1016/j.apenergy.2021.116893

Pérez-Salado Kamps, Á., Balaban, A., Jödecke, M., Kuranov, G., Smirnova, N. A., & Maurer, G. (2001). Solubility of single gases carbon dioxide and hydrogen sulfide in aqueous solutions of N-methyldiethanolamine at temperatures from 313 to 393 K and pressures up to 7.6 MPa: New experimental data and model extension. *Industrial and Engineering Chemistry Research*, *40*(2), 696–706. https://doi.org/10.1021/ie000441r

Plaza DH. Modeling of Carbon Dioxide Absorption Using Aqueous Monoethanolamine, Piperazine and Promoted Potassium Carbonate. PhD Thesis, USA: University of Texas at Austin; 2011.

Plaza, J. M., & Rochelle, G. T. (2011). Modeling pilot plant results for CO_2 capture by aqueous piperazine. *Energy Procedia*, *4*, 1593–1600. https://doi.org/10.1016/j.egypro.2011.02.029

Posey, M. L., & Rochelle, G. T. (1997). *A Thermodynamic Model of Methyldiethanolamine-CO 2-H 2 S-Water*. https://pubs.acs.org/sharingguidelines

Rabensteiner, M., Kinger, G., Koller, M., Gronald, G., & Hochenauer, C. (2015). Investigation of carbon dioxide capture with aqueous piperazine on a post combustion pilot plant-Part I: Energetic review of the process. *International Journal of Greenhouse Gas Control*, *39*, 79–90. https://doi.org/10.1016/j.ijggc.2015.05.003

Rackett, H. G. (1970). Equation of State for Saturated Liquids. In *Journal of Chemical and Engineering Data* (Vol. 15, Issue 4). https://pubs.acs.org/sharingguidelines

Rochelle, G. T., Akinpelumi, K., Gao, T., Liu, C. T., Suresh Babu, A., & Wu, Y. (2022). Pilot plant results with the piperazine advanced stripper at NGCC conditions. *International Journal of Greenhouse Gas Control*, *113*. https://doi.org/10.1016/j.ijggc.2021.103551

Rochelle, G. T., Wu, Y., Chen, E., Akinpelumi, K., Fischer, K. B., Gao, T., Liu, C. T., & Selinger, J. L. (2019). Pilot plant demonstration of piperazine with the advanced flash stripper. *International Journal of Greenhouse Gas Control*, *84*, 72–81. https://doi.org/10.1016/j.ijggc.2019.03.014

Rochelle, G., Chen, E., Freeman, S., van Wagener, D., Xu, Q., & Voice, A. (2011). Aqueous piperazine as the new standard for CO_2 capture technology. *Chemical Engineering Journal*, *171*(3), 725–733. https://doi.org/10.1016/j.cej.2011.02.011

Suresh Babu, A., & Rochelle, G. T. (2022). Energy use of piperazine with the advanced stripper from pilot plant testing. *International Journal of Greenhouse Gas Control*, *113*. https://doi.org/10.1016/j.ijggc.2021.103531

Suresh Babu, A., & Rochelle, G. T. (2022). Process design of the piperazine advanced stripper for a 460 MW NGCC. *International Journal of Greenhouse Gas Control*, *115*. https://doi.org/10.1016/j.ijggc.2022.103631

~~Takht Ravanchi, M., & Sahebdelfar, S. (2014). Carbon dioxide capture and utilization in petrochemical industry: potentials and challenges. *Applied Petrochemical Research*, *4*(1), 63–77. https://doi.org/10.1007/s13203-014-0050-5~~

Van Wagener DH. Stripper Modeling for CO_2 Removal Using Monoethanolamine and Piperazine Solvents. PhD Thesis, USA: University of Texas at Austin; 2011.

van Wagener, D. H., & Rochelle, G. T. (2011). Stripper configurations for CO_2 capture by aqueous monoethanolamine and piperazine. *Energy Procedia*, *4*, 1323–1330. https://doi.org/10.1016/j.egypro.2011.01.190

Wang, M., Joel, A. S., Ramshaw, C., Eimer, D., & Musa, N. M. (2015). Process intensification for post-combustion CO_2 capture with chemical absorption: A critical review. In *Applied Energy* (Vol. 158, pp. 275–291). Elsevier Ltd. https://doi.org/10.1016/j.apenergy.2015.08.083

Wang, M., Lawal, A., Stephenson, P., Sidders, J., & Ramshaw, C. (2011). Post-combustion CO_2 capture with chemical absorption: A state-of-the-art review. *Chemical Engineering Research and Design*, *89*(9), 1609–1624. https://doi.org/10.1016/j.cherd.2010.11.005

Wilke, C. R., & Chang, P. (1955). Correlation of diffusion coefficients in dilute solutions. *AIChE Journal*, 1(2), 264–270. https://doi.org/10.1002/aic.690010222

Wu, X., Wang, M., Liao, P., Shen, J., & Li, Y. (2020). Solvent-based post-combustion CO_2 capture for power plants: A critical review and perspective on dynamic modelling, system identification, process control and flexible operation. *Applied Energy*, *257*. https://doi.org/10.1016/j.apenergy.2019.113941

Xia, J., Pérez-Salado Kamps, Á., & Maurer, G. (2003). Solubility of H2S in (H_2O + piperazine) and in (H_2O + MDEA + piperazine). *Fluid Phase Equilibria*, *207*(1–2), 23–34. https://doi.org/10.1016/S0378-3812(02)00331-X

Zhang, Y., Freeman, B., Hao, P., & Rochelle, G. T. (2016). Absorber modeling for NGCC carbon capture with aqueous piperazine. In *Faraday Discussions* (Vol. 192, pp. 459–477). Royal Society of Chemistry. https://doi.org/10.1039/c6fd00030d

Zhang, Y., Sachde, D., Chen, E., & Rochelle, G. (2017). Modeling of absorber pilot plant performance for CO_2 capture with aqueous piperazine. *International Journal of Greenhouse Gas Control*, *64*, 300–313. https://doi.org/10.1016/j.ijggc.2017.08.004

Zhao, B., Liu, F., Cui, Z., Liu, C., Yue, H., Tang, S., Liu, Y., Lu, H., & Liang, B. (2017). Enhancing the energetic efficiency of MDEA/PZ-based CO_2 capture technology for a 650 MW power plant: Process improvement. *Applied Energy*, *185*, 362–375. https://doi.org/10.1016/j.apenergy.2016.11.009

Zhao, Z., Chong, K., Jiang, J., Wilson, K., Zhang, X., & Wang, F. (2018). Low-carbon roadmap of chemical production: A case study of ethylene in China. *Renewable and Sustainable Energy Reviews*, *97*, 580–591. https://doi.org/10.1016/j.rser.2018.08.008

Zhou, T., Shi, H., Ding, X., & Zhou, Y. (2021). Thermodynamic modeling and rational design of ionic liquids for pre-combustion carbon capture. *Chemical Engineering Science*, *229*. https://doi.org/10.1016/j.ces.2020.116076